Turbulence in Spatially
Extended Systems

ISBN 1-56072-120-0

ASYMPTOTIC SCALING IN TURBULENT COUETTE-TAYLOR FLOW

*J. Fineberg, D.P. Lathrop[1], and H.L. Swinney**
Center For Nonlinear Dynamics and Department of Physics,
University of Texas, Austin, Texas 78712

Abstract. Turbulent flow between concentric cylinders is studied in experiments for Reynolds numbers $800 < R < 1.23 \times 10^6$ for a system with radius ratio $\eta = 0.7246$. Although high precision torque measurements reveal a transition to wall-bounded shear flow at $R = 1.3 \times 10^4$, no range of Reynolds number exhibiting power law scaling of the torque is observed. However, the torque measurements above the transition are consistent with the form of asymptotic behavior predicted by scaling theory in this region. The observed Reynolds number dependence of the skin friction coefficient in turbulent pipe flow and flow over a flat plate are also consistent with this form.

1. Introduction

Turbulent flow is examined in a simple closed flow system: the flow between concentric rotating cylinders (the Couette-Taylor system). This work was partially motivated by recent experiments in another well known closed system: thermal convection at very high Rayleigh numbers [1]. In the latter experiments the heat transport in the system was found to exhibit regimes of well-defined power-law scaling as a function of the Rayleigh number. Our experiments were designed to measure the torque to high precision over a wide range of Reynolds number, well beyond that previously studied. The question of the existence of power-law scaling in this system is of a fundamental nature. For scales sufficiently well separated from the integral size of the system, if a universal turbulent flow exists, one might expect to see this type of behavior throughout the inertial range (since no underlying length scale exists in this regime). Contrary to these expectations, power-law scaling of mean flow quantities (such as the turbulent drag in a system) with the Reynolds number is *not* observed experimentally [2] in typical *open-flow* systems such

[1]Present address: Council of Engineering, Yale University, New Haven, CT 06520

as pipe flow, duct flow or flow over a flat plate. We will demonstrate that the observed lack of scaling in all of these systems can be described as corrections to scaling, of the type observed in equilibrium systems in the vicinity of a critical point, where in the fluid systems the critical point occurs in the infinite Reynolds number limit. A more detailed account of our experimental results can be found in references [3] and [4].

The Reynolds number in a system with only the inner cylinder rotating (as in our work) can be defined as:

$$R = \frac{\Omega a(b-a)}{\nu}, \tag{1}$$

where Ω is the rotation rate of the inner cylinder, a and b are the radii of the inner and outer cylinders, and ν is the kinematic viscosity of the fluid. For low Reynolds numbers this system has been extensively studied [5, 6, 7, 8] and has been found to exhibit a well-defined sequence of bifurcations leading to weak turbulence and turbulent Taylor vortices (turbulent flow with large scale toroidal vortices reminiscient of Taylor vortices observed at low Reynolds number) [9, 10, 11].

Theoretical predictions for scaling of the torque T with the Reynolds number having the form $T \sim R^{5/3}$ have been proposed [12, 13, 14]. These predictions assume that the flow, for moderately high Reynolds number, is described by an inviscid core region of constant angular momentum density matched to laminar boundary layers at the inner and outer cylinders. The width of the two boundary layers is determined by the condition that the boundary layers be marginally stable to either Taylor vortices [12, 13] or Gortler vortices [14].

In the limit of infinite Reynolds number [3, 4] dimensional arguments of the Kolmogorov type predict scaling of the form $T \sim R^2$. The scaling exponent value of 2 is an upper limit. This result was recently derived directly from the Navier-Stokes equation by Doering and Constantin [15].

Measurements of the torque imposed on the system to achieve steady-state rotation have been recently performed [3, 4]. These measurements showed that contrary to the above predictions, no power law scaling of the torque with Reynolds number was observed. Although it is possible to fit the data to different scaling exponents over various ranges of Reynolds number, as in previous experiments [16, 17], the "local" scaling exponent α (where $T \sim R^{\alpha}$) is in actuality a monotonically increasing function of R. The largest observed value of α is well below the predicted limit of $\alpha = 2$.

The torque measurements do however reveal the existence of a well-defined transition in the flow. At a Reynolds number of $R_T = 1.3 \times 10^4$ the behavior of the torque with R changes sharply and above R_T the flow closely corresponds to flows observed in turbulent wall-bounded shear flows.

2. Experimental Results

The experiments were performed in an apparatus specially designed to measure the torque exerted by the fluid on the inner cylinder to high precision over a large range of Reynolds number. The following description of the apparatus will be brief. A more

detailed description can be found in reference [4].

The outer cylinder is polished, transparent Plexiglas (polymethylmethacrylate) with an inner radius $b = 22.085$ cm and an axial length of $L = 69.50$ cm. The apparatus has a stainless steel inner cylinder with radius $a = 16.000$ cm, giving the system a radius ratio $\eta = a/b = 0.7246 \pm 0.0001$ and an aspect ratio $\Gamma = L/(b-a) = 11.47$.

To minimize effects due to the finite axial size of the system, the torque is measured solely along the center portion of the inner cylinder. To this end, the inner cylinder is constructed in three sections of length 15.69 cm, 40.64 cm, and 15.69 cm, stacked axially and separated by thin (0.025 cm) gaps. The upper and lower sections are rigidly attached to the rotating drive shaft, which is directly coupled to the motor. The center section of the inner cylinder, which senses torque, is positioned on the shaft by two low torque precision bearings and driven by means of a single torque sensing arm. The deflection of the sensing arm resulting from the applied torque is measured to 0.1% accuracy by means of lock-in detection.

To achieve the desired accuracy in the torque measurements, five different mixtures of water and water-glycerol with different viscosities were used. Temperature regulation of the working fluid to 0.1°C was maintained by utilizing the rapid axial heat transport of the turbulent flow. The heat generated by the turbulent flow (up to 2 kW) was extracted through end rings that bound the working fluid axially.

The axial flow state was determined by means of Kalliroscope visualization [18]. At low R turbulent Taylor vortex states with 8, 10, 12 and 14 vortices were observed [19]. For $R > R_T$ only 8 and 10 vortex states were stable, and above $R = 1.75 \times 10^4$ only the 8 vortex state was observed until it disappeared at $R \sim 10^5$.

Measurements of the torque were made for axial states with 8 and 10 vortices. The torque measurements for different fluids in the overlapping Reynolds number ranges agreed within the 1% uncertainty caused by uncertainty in the value of the fluid viscosity and density. Measurements made for increasing and decreasing Reynolds number showed no hysteresis for either flow state.

Figure 1 compares the predicted and measured values of the nondimensionalized torque, $G \equiv T/\rho\nu^2 L$ (where T is the measured torque and L is the length of the torque-sensing inner cylinder section) for the 8 vortex state. The lack of agreement is evident.

To determine whether the torque is indeed of the form $G \sim R^\alpha$, we differentiate the data to determine the local slope over intervals of $\Delta \log_{10} R = 0.1$: $\alpha(R) = \partial(\log G)/\partial(\log R)$. In order to eliminate uncertainties in the viscosities of the different fluids used, the values of α were first computed separately for each individual run. The results of all of the runs were then averaged. Figure 2 presents the values of α for both the 8 and 10 vortex states.

As seen in the figure, there is *no* range of R where α is constant. For the 8 vortex data, α increases monotonically from $\alpha = 1.23$ to 1.87. The sudden change in $\partial\alpha/\partial(log_{10}R)$ at $R = R_T = 1.3 \times 10^4$ in the 8 vortex data and the discontinuity in α at $R = 1.0 \times 10^4$ for the 10 vortex data indicate the point where the flow undergoes a transition to wall-bounded shear flow [3, 4]. Surprisingly, the transition for both axial states occurs at the $\alpha = 5/3$ scaling exponent predicted by Marcus [12, 13] using a marginal stability

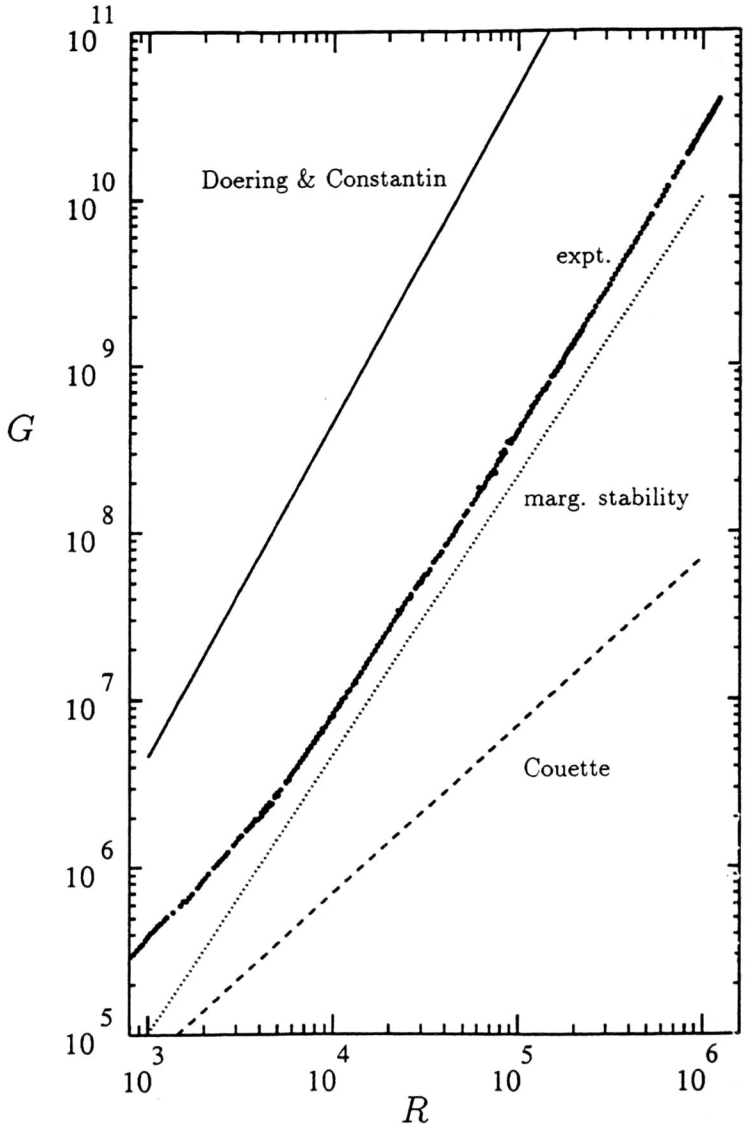

Figure 1: A comparison of the measured nondimensional torque for the 8 vortex state (from ref. [4]) with the marginal stability prediction $G \sim R^{5/3}$ [12,13], Couette flow torque [16], $G = 4\pi\eta\,[(1+\eta)(1-\eta)^2]^{-1}\,R$, and the Kolmogorov type prediction $G = \left[\pi\eta(1+\eta)/(8\sqrt{2}(1-\eta)^2)\right] R^2$ [27].

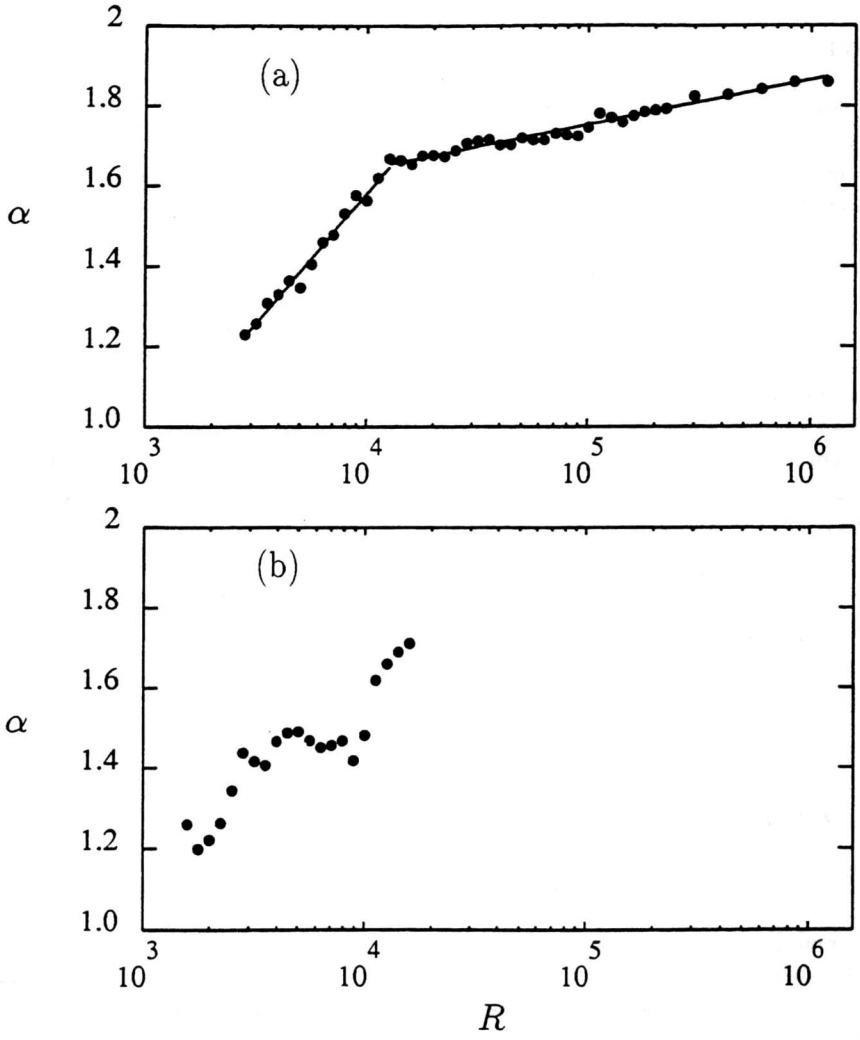

Figure 2: Local exponent for the torque, $\alpha = \partial(\log G)/\partial(\log R)$, calculated from torque measurements using least squares over a range $\Delta \log_{10} R = 0.1$: (a) measured for an eight vortex state (•); (b) measured for a ten vortex state (•). At $R = 2.0 \times 10^4$ the ten vortex state becomes unstabl e to the eight vortex state. For $R > 10^5$, turbulent Taylor vortices are not observed. (from ref. [4])

argument. (In Rayleigh-Benard convection an analogous argument correctly predicted the scaling exponent for the heat transport [20] in the "soft" turbulence regime [1, 21].)

3. Asymptotic Scaling

We now consider the flow above R_T where the system undergoes a transition to wall-bounded shear flow similar to turbulent pipe flow, duct flow and flow over a flat plate. The question of why power law scaling is not observed in this system naturally arises. As the Reynolds number of the system is raised to ever increasing values, one might expect the system's behavior to become independent of the details of the external boundaries which provide the forcing. At the same time the Kolmogorov length, the smallest scale in the system, shrinks rapidly to zero. Thus, for high enough Reynolds numbers, we would expect to see power law scaling characteristic of systems having no intrinsic length scale.

To understand why simple power law scaling is not observed in this system let us consider an analogy between high Reynolds number flow and the behavior of a equilibrium system in the region of a critical point. In a equilibrium system near criticality, the singular part of the free energy density F is a homogeneous function of a set of scaling fields $(\mu_1, \mu_2, \mu_3, ...)$ [22, 23]:

$$F(\mu_1, \mu_2, \mu_3, ...) = b^{-d} F(b^{y_1}\mu_1, b^{y_2}\mu_2, b^{y_3}\mu_3, ...),$$

where d is the dimension of the system. In this region, the behavior of the system for small b will be dictated by the "relevant" fields μ_i where the exponents $y_i > 0$. For a system with one relevant field μ_1 $(y_1 > 0 > y_2 > y_3 > ...)$ one has (choosing $b = \mu_1^{-1/y_1}$):

$$F(\mu_1, \mu_2, \mu_3, ...) = \mu_1^{d/y_1} F(1, \mu_2 \mu_1^{-y_2/y_1}, ...) \tag{2}$$

If μ_1 is sufficiently close to zero, expanding in $\mu_2 \mu_1^{-y_2/y_1}$ yields:

$$F(\mu_1, \mu_2, \mu_3, ...) \sim \mu_1^{d/y_1}(A + B\mu_2 \mu_1^{-y_2/y_1}) = \mu_1^{\zeta}(C_1 + C_2 \mu_1^{\lambda}) \tag{3}$$

where C_1 and C_2 are constants, $\lambda \equiv -y_2/y_1 > 0$ and $\zeta \equiv d/y_1 > 0$.

The first correction to scaling for finite values of μ_1 is given by Equation (3). Only as we asymptotically approach the critical point, $\mu_1 = 0$, is exact scaling of the function F observed.

Although there is no free energy for dissipative systems, we consider an analogous quantity, $P = T\Omega/V \sim GR$, the dimensionless power per unit volume V dissipated in our system. Let us now assume that in our system a critical point of the flow exists for infinite Reynolds number. In this system the quantities analogous to the scaling fields μ_i are the dimensionless variables R, $\delta \equiv 1 - \eta$ and $1/\Gamma$. We might then expect that as we approach the critical point $(R \to \infty)$:

$$P(R, \delta, 1/\Gamma) \sim l^{-d} P(Rl^{\zeta}, \delta l^{\beta}, \frac{1}{\Gamma} l^{\gamma}, ...). \tag{4}$$

We now assume that $\zeta > 0$ is the largest scaling exponent in Equation (4). As in Equation (3) we choose the scaling factor as $l = R^{-1/\zeta}$ and Equation (4) becomes:

$$P(R, \delta, 1/\Gamma) \sim R^{d/\zeta} P(1, \delta R^{-\beta/\zeta}, \frac{1}{\Gamma} R^{-\gamma/\zeta}, ...). \tag{5}$$

If Equation (5) is to make sense, both δ and $1/\Gamma$ must be relevant fields (i.e. $\beta > 0$ and $\gamma > 0$) so that as $R \to \infty$ the dissipated power flows to the fixed point corresponding to the limit of plane Couette flow ($\eta = 1$) with infinitely long plates (infinite aspect ratio):

$$P(R, \delta, 1/\Gamma)_{R \to \infty} \to R^{d/\zeta} P(1, 0, 0, ..). \tag{6}$$

For large enough values of R (assuming that P is an analytic function of δ and $1/\Gamma$) we can expand Equation (5) around this fixed point yielding:

$$P(R, \delta, 1/\Gamma) \sim R^{d/\zeta}(1 + aR^{-\beta/\zeta} + bR^{-\gamma/\zeta} + ...) \sim R^{d/\zeta}(1 + aR^{\lambda} + ...) \tag{7}$$

where $\lambda < 0$ is $max(\beta/\zeta, \gamma/\zeta)$. Thus for large Reynolds number:

$$G \sim \frac{P}{R} = R^{d/\zeta - 1}(a + bR^{\lambda} + ...) = R^2(a + bR^{\lambda} + ...) \tag{8}$$

where we have used the limiting value of $\alpha = 2$ for the leading exponent $d/\zeta - 1$ as derived in references [4] and [15].

A fit of the data for $R > R_T$ to Equation (8) yields $a = 0.0185 \pm 0.0008$ and $b = 4.94 \pm 1.0$ with the exponent $\lambda = -0.47 \pm 0.02$ (We estimate the errors by the values of the coefficients for a 10% increase in the rms value of the residuals to the fit.). The residuals from the fit (Fig. 3) show no systematic deviation of the data from the form given by Equation (8). For comparison, we also plot $(G_{Prandtl} - G)/G$ where $G_{Prandtl}$ is the torque predicted using the Prandtl -Von Karman type prediction for the torque derived in [4]. In addition, the local slope α obtained from Equation (8) is compared in Fig. 4 to the data and the slopes predicted by a marginal stability arguement [12] and the Prandtl - Von Karman type equation. The agreement with Equation (8) is clearly apparent.

The value of the scaling exponent, $\alpha = 2$, is only an *upper bound* deduced from the Navier-Stokes equations. As a consequence of the fractal structure of the dissipation volume, the actual exponent value could be smaller, perhaps as small as 1.9. We have examined the fit of our data to Equation (8) with the exponent α varied in the range from 1.8 to 2.2 and have found a shallow minimum in the variance at $\alpha = 2.04$, but at $\alpha = 1.95$ the variance is only 5% larger. Thus with our data we cannot rule out a value of α smaller than 2. Torque measurements extending to $R \sim 10^7$ with the accuracy of our data should however suffice to distinguish clearly between $\alpha = 1.95$ and $\alpha = 2$.

The good fit of our data to the scaling Equation (8) leads us to compare measured wall friction coefficients c_f [24] in other wall-bounded shear flows to this scaling form. In the infinite Reynolds number limit [25] we would expect these flows to exhibit the same asymptotic scaling as the Couette-Taylor system. Thus (since c_f is, by definition [24], normalized by a factor of R^2) we expect that for large Reynolds number:

$$c_f \sim a' + b' R^{\lambda}. \tag{9}$$

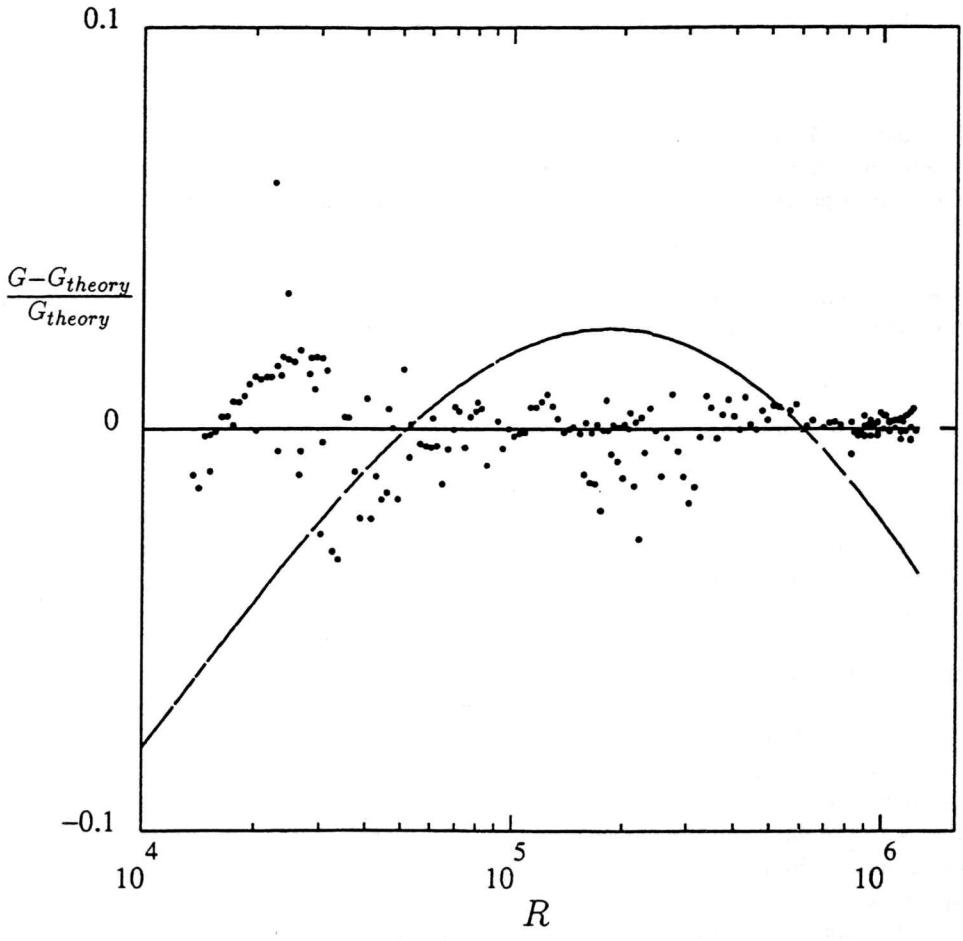

Figure 3: Residuals of the the best fit of the scaling equation, Equation (8), to the measured torque data using $a = 0.0185$, $b = 4.94$ and $\lambda = -0.47$. For comparison the Prantdl-Von Karman prediction [4], $1/\sqrt{c_f} = 1.52 log_{10}(R\sqrt{c_f}) - 1.63$, for Couette-Taylor flow is shown (solid line).

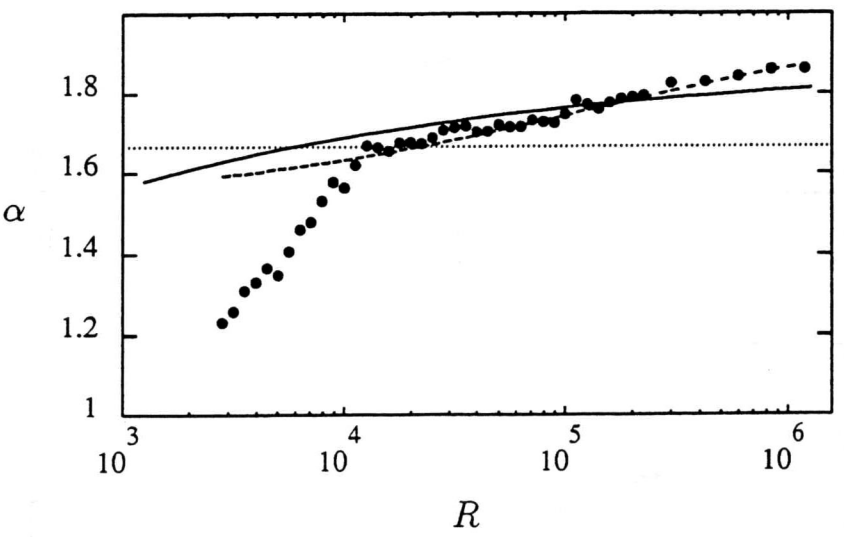

Figure 4: A comparison of the local slope α obtained from the measured torque data for an 8 vortex state (•) with predictions using Equation (8) (dashed line) and the Prandtl-Von Karman type theory (solid line).

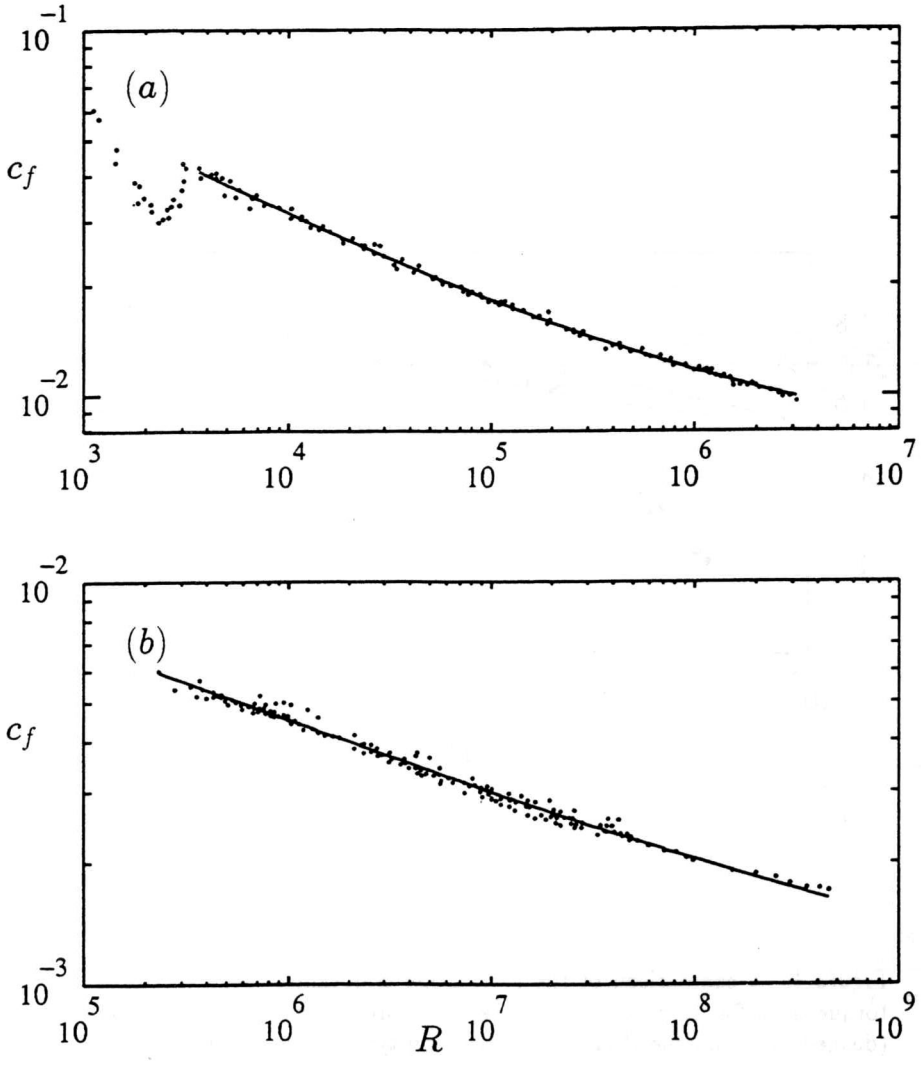

Figure 5: Measurements of the skin friction coefficient c_f for (a) pipe flow [26] and (b) flow over a plate [2] are compared with predictions of the form given by Equation (9) using $a' = 0.0055$, $b' = 0.45$ and $\lambda = -0.31$ for pipe flow and $a' = 0.00052$, $b' = 0.073$ and $\lambda = -0.21$ for flow over a flat plate.

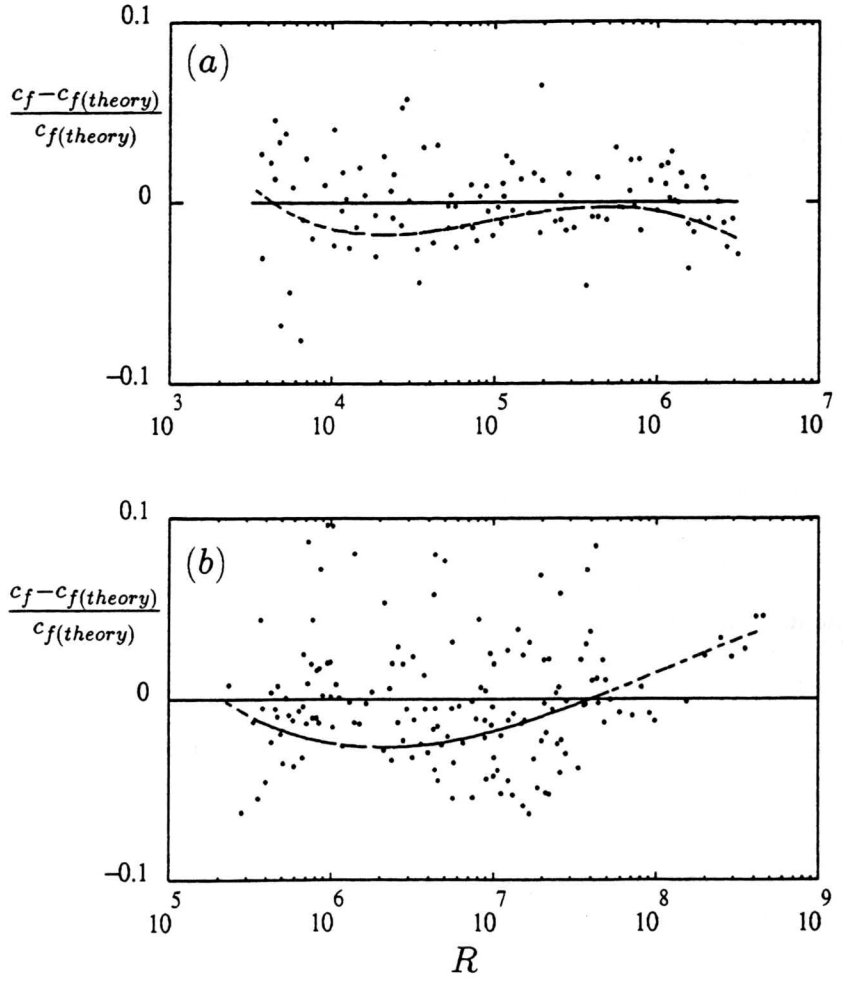

Figure 6: The deviations of the measured friction coefficient c_f (•)are compared with the predictions given by Equation (9) (solid line) for (a) pipe flow [26] and (b) flow over a flat plate. The parameters used are the same as in the previous figure. For comparison we include (dashed line) predictions for c_f given by the Prandtl-Von Karman formula, $1/\sqrt{c_f} = 2.0 log_{10}(R\sqrt{c_f}) - 0.8$, for pipe flow, and the Von-Karman-Schoenherr formula, $1/\sqrt{c_f} = 4.13 log_{10}(Rc_f)$ [28] for flow over a flat plate.

We would not expect correction exponents, λ, to be identical to that observed in Couette-Taylor flow since the scaling fields δ and $1/\Gamma$ may not be relevant for these flows.

In Figs. 5 and 6 we compare the measured friction coefficients of turbulent pipe flow [26] and flow over a flat plate [2] with fits of Equation (9) to the data. These data, like those for Couette-Taylor flow, exhibit no systematic deviation from Equation (9). For flow over a flat plate the best fit yields $a' = 0.00052$, $b' = 0.073$ and $\lambda = 0.21$ where, within a 10% variation in the rms value of the residuals to the fit, λ can vary by ± 0.11 and the corresponding values of the coefficients can change by as much as a factor of two. For the pipe flow data the best fit to Equation (9) yields $a' = 0.0055$, $b' = 0.45$, and $\lambda = -0.31$ where, again due to the relatively large scatter in the data, a 10% increase in the rms value of the residuals can change a' and b' by as much as 100% while the corresponding change in λ is ± 0.09.

The values of the correction exponent λ for both cases are consistent with the approach to the critical point being the same for both flows and, as in Couette-Taylor flow, no systematic deviation of the data from the prediction of Equation (9) is observed. Without further experiments we can not say whether or not the discrepancy in the exponents is significant.

In conclusion, we find that although no simple power law scaling for the torque $G \sim R^{\alpha}$ describes the observed results over any range of Reynolds number, measurements of the torque in turbulent Couette-Taylor flow and the skin friction coefficients for turbulent pipe flow and flow over a flat plate are consistent with corrections to asymptotic scaling at infinite Reynolds number.

In [3] and [4] measured flow quantities such as the turbulent diffusion coefficient, characteristic boundary layer time scales and probability functions were shown to be simple scaling functions of both R and the torque G. We would also expect these quantities to undergo scaling behavior in R alone in the asymptotic limit. By use of Equation (8) both their scaling exponents and corrections to scaling at finite values of the Reynolds number could be obtained.

We would like to acknowledge helpful discussions with J. Swift. This work is supported by ONR Grant No. N000014-89-J-1495.

* Electronic mail: swinney@chaos.utexas.edu

References

[1] B. Castaing, G. Gunaratne, F. Heslot, L. Kadanoff, A. Libchaber, S. Thomae, X.-Z. Wu, S. Zaleski, and G. Zanetti, *J. Fluid Mech.*, **204** 1 1989.

[2] H. Schlichting, *Boundary - Layer Theory* (Seventh Ed.) p. 598, p.639 and p. 641, McGraw-Hill, New York, 1979.

[3] D. P. Lathrop, J. Fineberg, and H. L. Swinney, *Phys. Rev. Lett.*, **68** 1515 1992.

[4] D. P. Lathrop, J. Fineberg and H. L. Swinney submitted to *Phys. Rev.* **A** 1992.

[5] G.I. Taylor, *Phil. Trans. Roy. Soc.*, **A223** 289 1923.

[6] D. Coles, *J. Fluid Mech.*, **21** 385 1965.

[7] R.C. Di Prima and H.L. Swinney, *Hydrodynamic Instabilities and the Transition to Turbulence* p. 139 (ed. H. L. Swinney and J. P. Gollub), Springer Verlag, Berlin, 1985.

[8] K. Kataoka *Encyclopedia of Fluid Mechanics* vol. 1 p. 236 (ed. by N.P. Cheremisinoff), Gulf, Houston, 1986.

[9] P.R. Fenstermacher, H.L. Swinney, and J. P. Gollub, *J. Fluid Mech.*, **94** 103 1979.

[10] A. Brandstater and H.L. Swinney, *Phys. Rev.*, **A35** 2207 1987.

[11] J.P. Gollub and H.L. Swinney, *Phys. Rev. Lett.*, **35** 927 1975.

[12] P.S. Marcus, *J. Fluid Mech.*, **146** 65 1984.

[13] G.P. King, Y. Li, W. Lee, H.L. Swinney and P.S. Marcus, *J. Fluid Mech.*, **141** 365 1984.

[14] A. Barcilon and J. Brindley, *J. Fluid Mech.*, **143** 429 1984.

[15] C. R. Doering and P. Constantin, preprint (1992).

[16] F. Wendt, *Ingenieur-Archiv*, **4** 577 1933.

[17] P. Tong, W.I. Goldburg, J.S. Huang, and T.A. Witten, *Phys. Rev. Lett.*, **65** 2781 1990.

[18] P. Matisse and M. Gorman, *Phys. Fluids*, **27** 759 1984.

[19] A 0.1% solution of Kalliroscope flakes was introduced into the flow when it was necessary to differentiate between the different axial flow states.

[20] W.V.R. Malkus and G. Veronis, *J. Fluid Mech.*, **4** 225 1958.

[21] F. Heslot, B. Castaing, and A. Libchaber, *Phys. Rev.*, **A36** 5870 1987. See also refs. therein.

[22] F. J. Wegner, *Phys. Rev.*, **B5** 4529 1972.

[23] J. Swift and M. K. Grover. *Phys. Rev.* **A9** 2579 1974.

[24] The friction coefficient for Couette-Taylor flow is $c_f = G/R^2$, $c_f = 8\tau_w/\rho v^2$ for pipe flow where v is the centerline flow velocity, and for flow over a flat plate $c_f = 2\tau_w/\rho v^2$ where v is the flow velocity far from the plate and $\tau_w \equiv \rho\nu\,|\partial u/\partial r|_{r=wall}$ is the wall shear stress.

[25] The Reynolds numbers used for comparison are $R = \bar{u}d/\nu$ for pipe flow (where d the diameter of the pipe) and $R = u_\infty x/\nu$ for flow over a flat plate (where x is the distance from the leading edge of the plate) [2].

[26] J. Nikuradse, *Forschung Arbeit Ingenieur-Westfalen* **356** 36 1932.

[27] C. Doering (private communication).

[28] H. Schlichting, *Boundary - Layer Theory* (Seventh Ed.), McGraw-Hill, New York, 1979. p. 611 for flow over a flat plate and p. 641 for pipe flow.